ChemComm

Capacitive Deionization System with Ultra-high Salt Adsorption Performance: From Lab Design to Agricultural Applications

Journal:	*ChemComm*
Manuscript ID	CC-FEA-07-2023-003206.R1
Article Type:	Highlight

ARTICLE

Capacitive Deionization System with Ultra-high Salt Adsorption Performance: From Lab Design to Agricultural Applications

Received 00th January 20xx,
Accepted 00th January 20xx

DOI: 10.1039/x0xx00000x

Rui He,[a,†] Yongchang Yu,[b,†] Lingchen Kong,[b] Xitong Liu[b]* and Pei Dong[a]*

Capacitive deionization is an emerging water desalination technology for industrial applications. Recent advancements in electrode design and system development have led to the reporting of ultra-high salt adsorption performance, benefiting its potential application in agricultural water treatment at a potentially low cost. In this study, we provide a comprehensive summary of the porous electrode design strategy to achieve ultra-high ion adsorption performance, considering factors such as experimental parameters, chemically-tuned material properties, redox chemistry and smart nanoarchiteture for future electrode design. Furthermore, we endeavor to establish a correlation between capacitive deionization (CDI) technology and its applicability in the agricultural sector, specifically concentrating on water treatment with an emphasis on undesirable ions associated with salinity, hardness, and heavy metals, to achieve harmless irrigation. Additionally, to ensure the efficient and cost-effective application of CDI systems in agriculture, a thorough overveiew of the literature on CDI cost analysis is presented. By addressing these aspects, we anticipate that ultra-high salt adsorption CDI systems hold great promise in future agricultural applications.

1. Introduction

Water usage in agriculture accounts for 70% of total freshwater withdrawal on a global scale and 80% of total freshwater withdrawal in the United States, highlighting the importance of efficient agricultural water utilization for food production.[1] Ensuring the quality of water used for irrigation is essential as it can directly impact crop health and productivity.[2] Water pollution caused by organic, inorganic, and biological pollutants[3–5] poses a challenge in maintaining appropriate water quality for irrigation purposes. Dissolved ions in water play a critical role in determining water quality, with certain elements like boron, arsenic, and uranium having adverse effects on crop growth and productivity if present in excessive amounts. [3,6,7] Thus, the removal of ions from brackish water is significant in agricultural areas to ensure optimal crop growth and mitigate potential challenges associated with water pollution.

Currently, a variety of water desalination technologies have been developed to address the removal of ions from brackish water, including chemical treatment,[8] thermal driven technologies such as multi stage flash[9] and pressure driven technologies like reverse osmosis.[10] These advancements are poised to have a significant impact on agricultural applications. However, these technologies have their limitations such as the generation of secondary waste, high energy assumption associated with thermally driven technologies, and membrane fouling challenge.[11,12] In light of these limitations, capacitive deionization (CDI) has emerged as a promising alternative.[13] For its potential in addressing the challenges associated with ion removal from brackish water, CDI has gained attention and extensive research over the past decades.

CDI is a novel electrochemical adsorption method utilized for removing ions from brackish water.[14] During the adsorption process, the charged electrode attracts oppositely charged ions (Fig. 1), which are subsequently released and stored separately during desorption. Salt adsorption capacity (SAC) is the essential parameter used to evaluate the salt adsorption performance, calculated by dividing the mass of salt being adsorbed by the total mass of the electrodes.[15] In recent years, a wide range of conditions related to salt adsorption have been extensively studied. These conditions include system operating parameters such as cell voltage, cycle duration, temperature, saline solution flow rate.[16,17] Moreover, the properties of the electrode, such as porous structure and electrical properties, have been thoroughly investigated.[11] Additionally, the characteristics of ions within the electrolyte, including their valence and ion radius, have also been taken into account.[15,18,19] Extensive research has been

[a] Department of Mechanical Engineering, George Mason University, Fairfax, VA 22030, USA.
[b] Department of Civil and Environmental Engineering, George Washington University, Washington, D.C., 20052, USA
† The authors contribute equal to this work.

conducted to develop advanced electrode materials aiming at achieving high SAC value. These advanced electrode materials, including but not limited to iron-nitrogen-carbon, tungsten oxide ($W_{18}O_{49}$)/graphene composite electrode, and aluminum oxide coated electrode, displayed a superior salt adsorption performance than commercial activated carbon.[20–23] Inspired by the excellent ion removal property, a growing number of works focus on developing the ultra-high salt adsorption CDI system to further enhancing the potential for agricultural industrial applications.[24]

This mini-review first presents a comprehensive review of ultra-high performance of different electrodes used in CDI. In addition, we discuss the strategies for designing electrodes by chemical activation and redox reaction with enhanced salt adsorption performance. Additionally, the application of CDI in agricultural areas for salinity, water hardness and heavy metal removal is investigated. Furthermore, an overview of the cost analysis studies of CDI for agricultural applications is presented. This mini-review will also contribute to the understanding and potential implementation of CDI technology in agricultural areas.

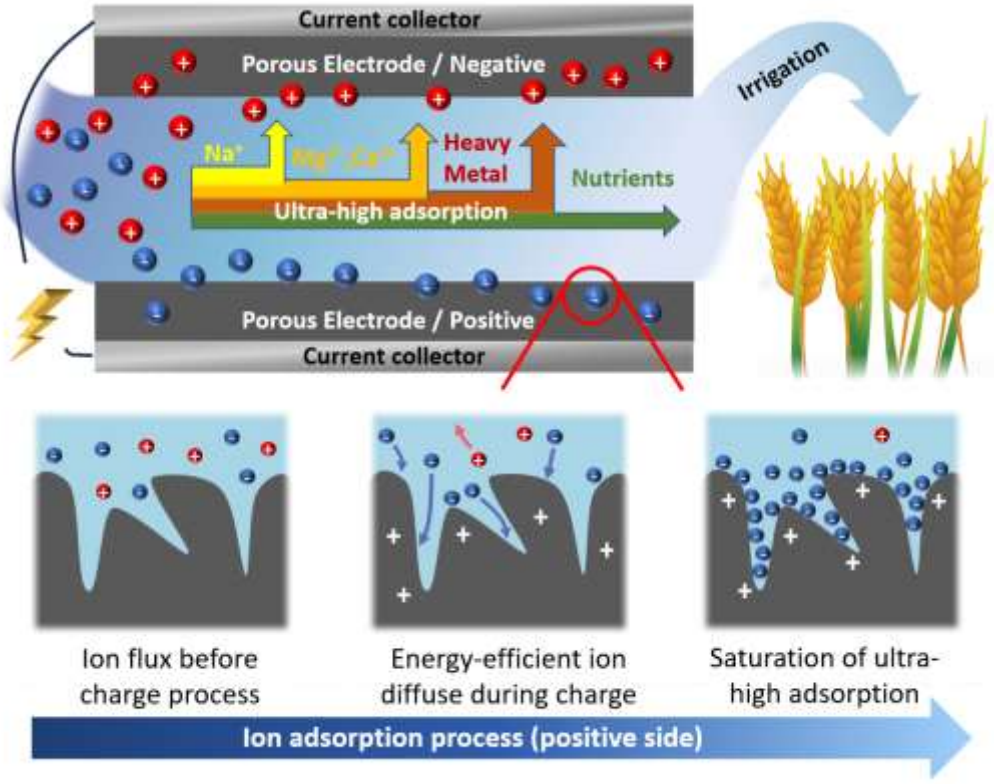

Figure 1. Schematic illustration of CDI adsorption process and its application in agricultural water treatment.

2. Ultra-high performance CDI lab design

In recent years, there has been a significant focus on achieving ultra-high SAC in CDI system for electrode design and future industrial applications. Over the last decade, the reported ultra-high SAC has been increased from less than 5 mg g^{-1} to over 100 mg g^{-1}.[25,26] In this section, the mechanism of ultra-high CDI performance is analyzed by summarizing the relevant papers that claimed "ultra-high" or reported a SAC higher than 50 mg g^{-1}. Furthermore, the design strategy of future electrode with ultra-high salt adsorption performance is provided.

2.1 Experimental setup design

CDI is an electrochemical method used to remove the ions from brackish water. It involves the utilization of a pair of porous electrodes, which are installed into a CDI cell connected to the saline solution and a power supply. The desalination occurs when a voltage is applied to the electrode after the saline solution flows into the cell and immerses the electrode (Fig. 2a). During this process, the ions are effectively absorbed onto the electrode surface, leading to the removal of salts from the solution (Fig. 1). Nowadays, tremendous efforts have been invested in optimizing materials design, salt adsorption kinetic to enhance the ion adsorption property. Meanwhile, researchers also study the experimental parameters to understand their roles in CDI performance.

During salt adsorption process, it is generally observed that a higher initial saline solution concentration could lead to a higher SAC. This is attributed to the presence of a greater number of ions in the solution at high concentration, which benefits the ion

transport and increases the salt adsorption performance. For example, when NaCl concentration increase from 250 ppm to 1000 ppm, the SAC of a hierarchical porous carbon electrode increases from 24 to 83 mg g^{-1} (Fig. 2b).[16] Meanwhile, voltage also have an impact on the final SAC result. Usually, a higher voltage will provide a strong electric field, which benefits the salt adsorption behavior.[27] For example, when increase the voltage from 1.2 V to 1.8V, the SAC of a NTP/C electrode reaches approximately 35 mg g^{-1} according to Fig. 2c.[17] Similarly, the SAC of $Ti_2C_2T_x$ MXene electrode exhibits an approximately 25% enhancement by increasing the voltage from 1.2 to 1.6 V.[28] However, the voltage needs to be carefully designed to prevent the decomposition of water. Chen et al.[27] studied the relation between voltage and SAC by using a composite electrode that are comprised of NTP and MXene prepared by autoclave, and an AC as another electrode for hybrid CDI system. The SAC increase from 26.0 (1.2V) to 128.6 (1.8V) mg g^{-1} in 1000 mg L^{-1} saline solution without water electrolysis observed.

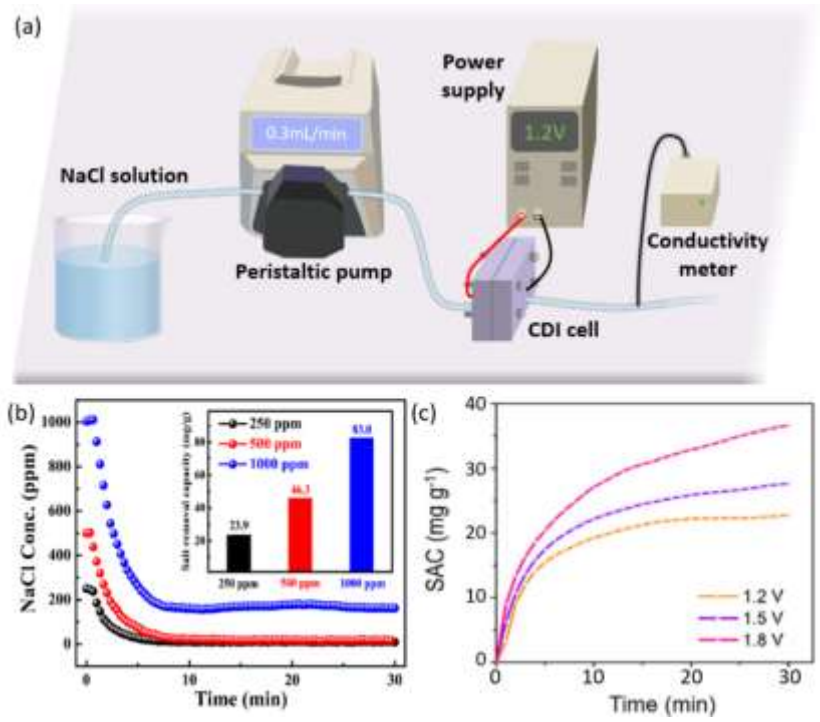

Figure 2. (a) Schematic illustration of single-pass mode CDI experimental setup.[14] Copyright 2022 Wiley. (b) The SAC of carbon electrode under different NaCl concentration.[16] Copyright 2020 American Chemical Society. (c) The SAC of electrode under different applied voltage.[17] Copyright 2023 American Chemical Society.

For some ultra-high related CDI papers, it is noticeable that excellent SAC results were reported under conditions of high cell voltage and high feed water concentration. These CDI could be used effectively when the parameters match the actual application conditions. For example, the desired voltage and the initial salinity of the feed could closely reflect environmental conditions. In specific application like agriculture irrigation water treatment, it is important to set the initial concentration of the wastewater to a value that closely resembles the concentration of brackish groundwater or agricultural wastewater found in the target environment. Additionally, the water after desalination should meet the relevant requirements such as acceptable electrical conductivity and total dissolved solids (TDS) for irrigation purpose, while the energy assumption is also significant to be considered.[29,30] Therefore, from the application evaluation, it is critical to specifically design the experimental conditions instead of using the most commonly used ones.

2.2 Non-faradaic electrode design strategy

In non-faradaic electrode for CDI, also named capacitive electrode, ion adsorption occurs through the formation of electrical double layers (EDLs). The electrode becomes charged when a voltage is applied, attracting oppositely charged ions from the saline solution. The process leads to the formation of a stern layer and a diffuse layer.[15] The electrode design typically focuses on aspects including surface properties and electrical performance.

2.2.1 Advanced materials with enhanced specific surface area and pore size distribution. Surface properties, including specific surface area (SSA) and pore size distribution play an important role for effective salt adsorption in CDI. In general, the greater the surface area, the more ions can be attached to the surface of charged electrode and be adsorbed, while the porous structure determines the EDLs when the charge is given to the electrode. This is why porous carbon materials are the most popular electrode material for CDI.[14] In addition to directly select the materials with high SSA, activation of carbon substrate is a common method to further increase the surface area. This involves creating a porous structure by removing part of carbon substrate at the nanoscale, which would reduce the total weight while maintaining the overall volume.

During the activation process, the extra porous structure on the surface of carbon substrate will be largely created by the reaction between the activating agent and carbon. The created porous will provide additional surface area to the total carbon electrode, further improving the salt adsorption performance. For example, Liu et al.[31] prepared a biochar using an agricultural waste - lotus leaf as precursor for water desalination (Fig. 3a). After activation by potassium hydroxide (KOH) followed by equation 1 and 2,[14] the surface area of carbon increased from 4.5 $m^2 g^{-1}$ to 4482 $m^2 g^{-1}$, leading to the ultra-high SAC of 65 mg g^{-1}. According to scanning electron microscope (SEM) images, Zhang et al.[16] obtained a porous electrode using α-cellulose and potassium bicarbonate ($KHCO_3$) as precursor and activating agent (Fig. 3b,c). After thermal activation at 800 °C, the BET surface area reached 1911.9 $m^2 g^{-1}$ (Fig. 3d), which is more than twice than the one without activation and leading to an 83 mg g^{-1} SAC performance. Meanwhile, large amount of micropores (pore width <2 nm) and mesopores (pore width 2-50 nm) are observed after activation process (Fig. 3e). In addition to KOH and $KHCO_3$, some other activating agents that could react with carbon at high temperature have been explored and utilized in water desalination area, including $ZnCl_2$, CO_2, H_3PO_4.[32–35] As a result, how to find a high efficient activating agent, in other words, to achieve the high surface area carbon using less amount of reagents and low temperature needs to be studied in the future. In summary, activation process is one prominent method to increase the surface area and fabricate the designed pore-size distribution, further leading to an ultra-high salt adsorption performance of carbon electrodes, especially for those prepared by the carbonization of natural agricultural waste. By tuning the amount of activating agent and activation temperature, the extent of pore formation can be controlled, which further modifies the surface properties of carbon electrodes. The surface area of the carbon electrode maximized by activation enhances the SAC to improve the desalination performance, making these porous carbon electrodes highly desirable for efficient desalination application.

$$6KOH+2C \rightarrow 2K+3H_2+2K_2CO_3 \quad (1)$$

$$K_2CO_3+2C \rightarrow 2K+3CO \quad (2)$$

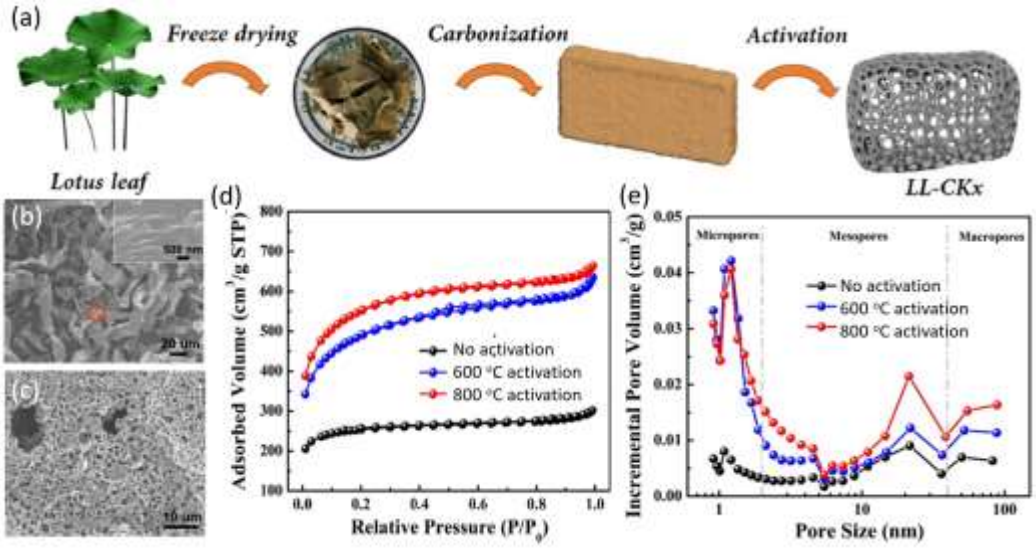

Fig. 3 Activated carbon (AC) electrode for CDI. (a) schematic illustration of activated lotus leaf carbon preparation.[31] Copyright 2020 Elsevier. SEM image of α-cellulose (b) before and (c) after activation.[16] Copyright 2020 American Chemical Society. (d) N_2 adsorption/desorption curve of α-cellulose carbon.[16] Copyright 2020 American Chemical Society. (e) Pore size distribution of activated carbon.[16] Copyright 2020 American Chemical Society.

2.2.2 Advanced materials with enhanced electrical property. EDL and ion transport pathway are significant factors need to be analyzed for electrode design in CDI. When a charge is applied, the pair of electrodes will exhibit positive and negative charge, resulting in the attraction of oppositely charged ions on the electrodes (Fig. 1). This leads to the formation of a Stern layer, which is directly adjacent to the surface of the porous structures, and a diffuse layer further away from the electrode surface, as shown

in Fig. 4a.[36] Meanwhile, the diffuse layer overlaps within the micropore (pore width <2 nm) structure according to modified Donnan model (Fig. 4b).[19] A higher specific capacitance, as well as a fast ion transport pathway are directly linked to the superior salt adsorption performance. To achieve ultra-high salt adsorption, a variety of advanced materials with excellent electrical properties have been utilized in electrode fabrication. For example, N-doped graphene sponge was prepared using freeze drying and annealing in NH_3, for which exhibits a 286.86 F g^{-1} specific capacitance compared to 204.66 F g^{-1} of graphene sponge without N doping. The superior capacitance is contributed to the inclusion of N element, which could increase the electrical conductivity and improve the hydrophilic of the graphene electrode, leading to a SAC of 21 mg g^{-1}.[37] This SAC result is claimed to be the highest reported value reported in 2015 using carbon electrode.[37] Xu et al.[38] developed a MOF tube structure by grow zeolitic imidazolate framework (ZIF) on polyacrylonitrile (PAN) nanofibers. After dissolving PAN, a MOF electrode is obtained with hollow tube structure. The unique morphology supplies supplementary SSA and efficiently shortens the ion transport pathway. Meanwhile, the N dopant largely enhances the electron transfer and improves the SAC. The simulated SAC result is 56.9 mg g^{-1} according to Langmuir isotherm in 10 mM NaCl solution.[38] Xing et al.[39] demonstrate that particle size influences the electrical properties of the material. By controlling the particle size of ZIF from 100 nm to 450 nm, they observe that smaller particles exhibit a shorter charge transfer pathway. Additionally, the incorporation of conductive carbon powder improves the ion transfer bridge properties for smaller MOF particles. The electrode prepared with 100 nm particles showed a maximum SAC of 28.54 mg g^{-1} (Langmuir method) in a 40 mM saline solution with a voltage of 1.2 V. This finding highlights the importance of particle size control in optimizing the electrical properties of electrodes design strategy for CDI applications.

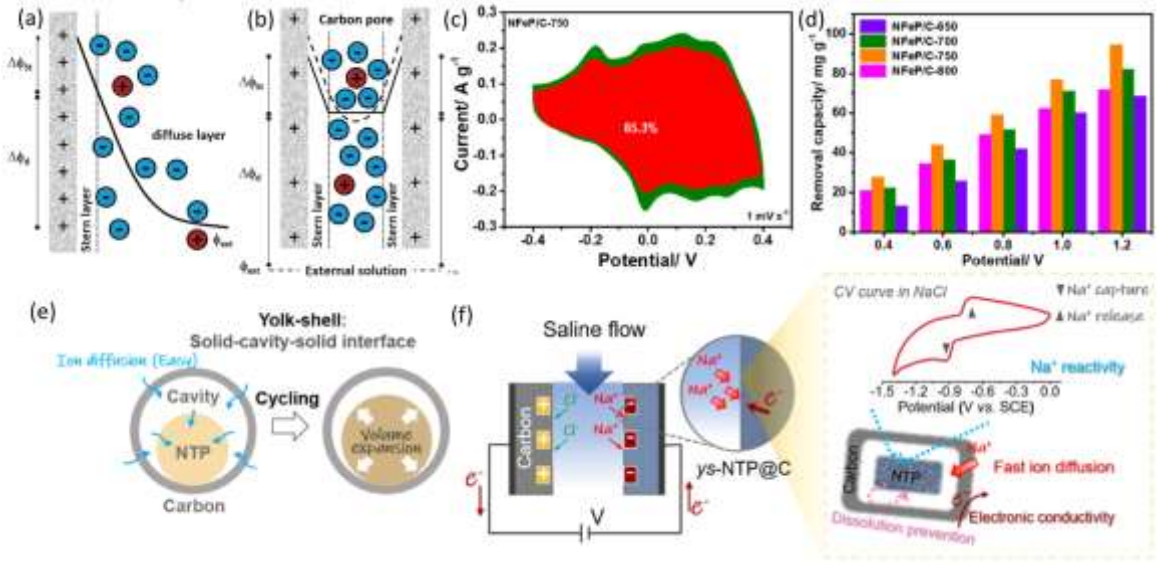

Figure 4. Electrical properties of electrodes in CDI. (a) The formation of EDLs by Gouy-Chapman-Stern model and (b) modified Donnan model.[19] Copyright 2015 Royal Society of Chemistry. (c) Faradaic NFeP/C electrode CV curve, red and green areas indicate the capacitive and diffuse controlled capacity, respectively.[40] (d) NFeP/C electrode SAC results.[40] Copyright 2021 Elsevier. (e) Yolk-shell nano architecture design illustration.[17] (f) NTP/Carbon yolk shell electrode and its faradaic salt adsorption performance.[17] Copyright 2023 American Chemical Society.

The utilization of advanced materials with exceptional surface and electrical properties has shown promise in achieving ultra-high SAC, as summarized in Table 1. However, transitioning these materials from lab-scale to industrial applications, such as agriculture brackish water desalination, requires careful consideration of feasibility, cost-effectiveness, energy cost, and other practical factors (details in section 3 and 4). By addressing these considerations, the successful integration of advanced materials can lead to practical and sustainable solutions for water desalination.

Table 1 Summary of works claimed ultra-high adsorption using carbon electrodes.

Electrode material	Specific Surface Area [m^2 g^{-1}]	Capacitance [F g^{-1}]	Voltage [V]	NaCl salinity [mg L^{-1}]	SAC [mg g^{-1}]	Published year	Reference
Graphene	305	57	1.5	(Conductivity 106 μS cm^{-1})	4.95	2014	[25]

N-doped graphene sponge	526.7	286.86	1.2	500	21	2015	[37]
Nonporous graphene	445	~200	1.6	500	17.1	2016	[41]
Graphene hydrogel	517	~35	2	500	49.34	2018	[42]
N-doped GO/CNT	83.6	34.1	(100 mA g^{-1})	2500	75	2019	[43]
lotus leaf carbon	4482	225	1.6	2000	65	2020	[31]
P, N doped carbon	1336	228	1.2	1000	39.34	2021	[44]

2.3 Faradaic electrode design

Faradaic electrode, in contrast to non-faradaic electrode, utilized redox reactions for ions storage. The electrodes typically incorporate intercalation materials that can store specific ions present in brackish water. Taking NaCl as an example, metal- or metal oxide-based intercalation materials such as $NaTi_2(PO_4)_3$ (NTP), $Na_{0.44}MnO_2$ (NMO), $Na_4Ti_9O_{20}$ (NTO) are commonly used for Na^+ ion capture, while intercalation materials like bismuth oxychloride (BiOCl), iron oxychloride (FeOCl) are popular choices for Cl^- ions as described by the equations below:

$$NaTi_2(PO_4)_3+2Na^++2e^- \leftrightharpoons Na_3Ti_2(PO_4)_3 \quad (3)$$

$$Na_{0.44-x}MnO_2 +x\ Na^++xe^- \leftrightharpoons Na_{0.44}MnO_2 \quad (4)$$

$$Na_4Ti_9O_{20}+9Na^++9e^- \leftrightharpoons Na_{13}Ti_9O_{20} \quad (5)$$

$$3BiOCl + 3e^- \leftrightharpoons Bi + Bi_2O_3 + 3Cl^- \quad (6)$$

Recently, several groups have reported the ultra-high SAC by using faradaic intercalation material as electrode. For example, Wang et al.[40] reported a $Na_3Fe_2(PO_4)_3$ (NFeP)/C electrode through a two-step preparation method: $NH_4H_2PO_4$, $C_6H_8O_7$, $Fe(NO)_3$ and $NaNO_3$ were mixed and autoclaved, then calcination to directly obtain NFeP/C composite. By tuning the calcination temperature, they found 750 °C is the most suitable one to obtain the large surface area electrode, which performed a 85.3 % capacitive charge storage (also known as pseudocapacitance) based on Dunn's approach,[45] and a 97.8 mg g^{-1} adsorption behavior in 200 mg L^{-1} NaCl solution (Fig. 4c and d).[40] Moreover, a sol-gel method was used to prepare $Na_3V_2(PO_4)_3$ (NVP)/C electrode with an open framework strucutre.[46] The ultra-high salt adsorption (137.2 mg g^{-1}) was observed under 1V and 100 mM NaCl concentration experimental conditions. Meanwhile, Chen et al.[47] reported a superior salt adsorption performance by combining NMO and BiOCl electrode into one CDI system to achieve a dual-ions faradaic deionization. The SAC of the electrode reached 68.5 mg g^{-1} under 100 mA g^{-1} constant current charge process. Compared to metal- or metal oxide- based faradaic materials and their redox reaction kinetics, MXene, as another advanced 2D material, is also applied as an intercalation electrode in CDI. Due to its special layer-by-layer structure, MXene stores the ions between the layers by pseudocapacitive intercalation mechanism.[24] Jie Ma et al.[28] used $Ti_3C_2T_x$ as a binder-free electrode. Although the surface area of the electrode is only 2.1 m^2 g^{-1}, a strong specific capacitance (127.76 F g^{-1}) at 100 mA g^{-1} owned by MXene guarantees its high salt adsorption performance, while the pseudocapacitive charge transfer have a major impact on its desalination performance other than EDL capacitance.[48] The hydrophilic electrode further provide a surface with high wettability, and therefore reduce the ion transport pathway and enhance the desalination performance (68 mg g^{-1}).[28] Chen et al.[27] also reported a Ti_3C_2 MXene derived NTP hybrid electrode by mixing the prepared MXene and other chemical components and autoclaved together. The hybrid electrode was found to have 128.6 mg g^{-1} ultra-high adsorption property.

Recent works have found that nanoarchitecture design has emerged as a promising approach to enhance the SAC of faradaic electrodes. Researchers have explored novel electrode structures with improved electron transfer and ion storage capabilities. For example, Liu et al.[17] developed a yolk-shell NTP/C electrode from MOF/covalent organic polymer (COP) precursor (Fig. 4e). The carbon shell nano structure efficiently improves the total electron transfer, and prevents the dissolution of NTP during the charge period (Fig. 4f). The electrode achieved an ultra-high SAC of approximately 200 mg g^{-1} at 100mA g^{-1} under a constant current method using a 600 mM NaCl solution. Similarly, Zhang et al.[49] successfully synthesized a N,P-doped carbon/MXene electrode with core-shell nanostructure through the calcination process of MXene/ZIF-67 precursor. Compared to pure MXene, the C/MXene exhibited over 60 F g^{-1} capacitance at current density 0.5 A g^{-1}. The heterostructure structure effectively resolved the stacking issue of MXene, leading to significantly improved electrical conductivity of the whole electrode. The core-shell electrode has a maximum SAC value of 74.8 mg g^{-1} (Langmuir method) with 1.4V voltage applied.

The faradaic electrode exhibits an ultra-high SAC due to its redox reaction even though with a low surface area as summarized in Table 2. Therefore, in the design of such electrodes, carefully controlling the amount of intercalation materials, as well as the selection of suitable faradaic materials, becomes crucial for future practical applications. Especially for agriculture brackish water treatment, when addressing the removal of hardness or heavy metal ions other than NaCl, thorough consideration must be given to the appropriate choice of faradaic intercalation materials. On the other hand, the development of smart nano architecture design offers solutions to key challenges faced by faradaic materials in CDI systems. By addressing issues like material dissolution during charge and the stacking problem of certain materials like MXene, these designs ensure the stability and high performance of the electrodes, leading to ultra-high SAC results. Furthermore, exploring diverse material combinations and optimizing their properties holds the potential to further enhance SAC efficiency. Therefore, as we move towards practical applications in agricultural areas, it becomes crucial to explore methods for simplifying the fabrication process of these electrodes.

Table 2. Summary of faradaic electrode with ultra-high SAC performance.

Electrode material	SSA [m^2 g^{-1}]	Capacitance [F g^{-1}]	Voltage [V]	NaCl salinity [mg L^{-1}]	SAC [mg g^{-1}]	Reference
NTP/MXene//AC	24.3	-	1.8	1000	128.6	27
NTP/C//$LiMn_2O_4$/C	10.23	-	1.8	1170	140.03	26
NTP/C//AC	246.7	164.8	1.8	1000	167.4	50
NFeP/C//AC	46.2	163.2	1.2	500	94.5	40
C/NTO//AC	193.65	153.34	1.4	1000	66.14	51
BiOCl/CNF	-	846.12	1.2	3000	124	52
CuFe@NiFe	-	-	(Current density 0.5 mA cm^{-2})	2925	71.8	53
Bismuthene/MXene	25	332	1.4	1170	95.7	54
$Ti_3C_2T_x$	2.1	127.76	1.2	585	68	28
TiO_2/Ti_3C_2	50.74	207	1.2	500	64.32	55

Noticeably, the oxidation of electrode is a common faradaic reaction in CDI. The oxidization process generates hydrogen peroxide and decreases the stability of the electrode, which negatively affects the ion adsorption process.[56] To address this challenge, the advanced material that can reduce the oxidation process needs to be carefully designed. For example, using MOFs as precursors to prepare carbon electrodes has been found to exhibit excellent oxidation reduction reaction properties.[56] Alternatively, designing oxidation-resistant MOFs offers another direction to prevent negative faradaic reactions.[57] Moreover, Zhang et al. [58] developed a MXene/covalent organic framework (COF) electrode in a heterostructure. The composite material exhibited over 80% SAC retention after 100 cycles, while the SAC reduction rate for pure MXene electrode is over 50% within 20 cycles charge/discharge period. Thus, the design of electrode materials with high oxidation reduction reaction performance is crucial for maintaining a stable salt adsorption process, guaranteeing the long-term usage of CDI in practical water treatment.

As a summary for future electrode design, several crucial factors influence the salt adsorption performance of non-faradaic electrodes, primarily focusing on surface and electrical properties. Future advancements should encompass more accessible experimental techniques to create additional sites for ion absorption, shorten ion transport pathways during adsorption, and increase the area of ELDs. For instance, employing more efficient activating agents to enhance surface area, utilizing sacrificial materials to control porous structures, and innovating advanced materials with enhanced electrical properties are essential steps. On the other hand, faradaic electrodes rely on the specific interaction between intercalation materials and ions for high selectivity. Yet, wastewater often contains multiple ions, necessitating careful design to trim different harmful ions to the safe irrigation level. Thus, mixing various intercalation materials in one electrode could provide a solution. Furthermore, in lab-scale contexts, nanoarchitecture design has proven effective in enhancing faradaic electrode stability and electrical properties, warranting further exploration. Meanwhile, from an industrial perspective, cost-effective and viable electrode production is vital for agricultural application. By addressing these factors comprehensively, the next-generation electrodes can be successfully applied to agricultural water treatment.

3. CDI in agricultural applications

In recent years, CDI technology synergizes effectively with the agricultural sector due to the abundance of suitable materials that can be utilized to prepare the source of electrode materials for CDI. Numerous agricultural resources can be employed in the production of high salt adsorption and low-cost electrode materials, thereby establishing a complementary relationship between CDI and agriculture. On the other hand, CDI has emerged as a promising and emerging water treatment technology, particularly for brackish water desalination and ion-selective separations. This is of utmost importance, given the crucial role that desalination plays in meeting the growing water demands for agricultural irrigation, particularly in regions facing water scarcity. As a result, a clear link exists between CDI technology and its application in the agriculture domain. This section aims to establish the connection between CDI technology and its agricultural applications by summarizing relevant case studies and exploring the potential benefits and opportunities associated with combining their respective applications.

3.1 Agricultural-related sustainable CDI electrode

In the quest for sustainable solutions in agriculture, the utilization of biomass waste as a viable source for CDI holds great promise. Taking advantage of abundant, economical, and environmentally friendly agricultural waste, consisting primarily of carbohydrates, serves as a significant and renewable energy source with remarkable ion storage capabilities. Previous studies investigate the potential of coffee endocarp, macadamia nutshell, corncob, bagasse bottom, cassava peel ash, sunflower seed, and sawdust fly ash as precursors for producing agricultural waste converted carbon through thermal carbonization methods.[59–64] Thermal carbonization is typically conducted at high temperatures in the presence of protective gas to prevent biomass precursor oxidation, after which the CDI electrodes are manufactured. Li et al.[31] grounded the lotus leaf carbon to powder and mixed with 10 wt% carbon black and 10 wt% polytetrafluoroethylene (PTFE) to fabricate a porous carbon film by casting onto a graphite sheet. The obtained electrode exhibits an ultra-high salt adsorption performance as introduced in section 2.2. González-García et al.[65] produced a binder-free affordable activated bamboo biochar by directly carbonized bamboo materials without the addition of polymer binders. The produced biochar exhibited a nanostructure composed of highly disordered graphene-like layers, along with a relatively high surface area and micropore structures, making them suitable for use as electrodes in CDI. The utilization of agricultural waste for the preparation of carbon electrodes in CDI applications represents a green approach to agricultural recycling. Moreover, the modification of these carbon electrodes through activation and composite with advanced materials, as discussed in Section 2, proves to be an effective method for enhancing their salt adsorption performance to achieve ultra-high ion removal. This makes them highly suitable for irrigation water treatment. Therefore, the reuse of agricultural waste and the purification of agricultural feed water position agricultural-related carbon electrodes as a promising solution for future CDI applications in high salt adsorption for an environmentally friendly and cost-effective purpose.

3.2 Application of CDI technology for agricultural irrigation

CDI offers several key advantages for agricultural water treatment, including scalability, remote operation capability, and potential cost-effectiveness.[66] CDI's ability to selectively remove TDS optimizes energy consumption, making it a sustainable choice in agricultural water purification (Fig. 1). Meanwhile, its modular design allows for efficient resource utilization, and it can be powered by photovoltaic arrays from remote locations.[66] As a result, CDI is a promising technology to improve water quality for irrigation, enhance crop productivity, with potentially low maintenance and operating costs. Since in the real world, the concentration of the ions in groundwater is far below the one used in lab-scale as introduced in section 2,[3] the removal efficiency is also used to studies to represent the salt removal properties.

3.2.1 Salinity. Desalination is crucial for addressing agricultural irrigation scarcity, and CDI offers a promising solution. By utilizing porous electrodes, CDI removes harmful ions from wastewater to reduce salinity. Additionally, membrane capacitive deionization (MCDI), which utilizes ion-selective membranes attached to the porous electrode surface, has gained popularity in agricultural irrigation water treatment.[67] This technology offers improved performance in terms of ion removal, energy efficiency, and selectivity, making it a preferred choice for agricultural applications Elshafei et al.[68] conducted a study to assess the viability of desalinating brackish water for irrigation purposes by designing a modular unit with a production capacity of 32 m^3 d^{-1} specifically for use in a 9 m*40 m greenhouse. The feed brackish water had a TDS concentration of 4000 ppm, while the desired TDS level for irrigation was set at 800 ppm. In general, the recommended range is less than 450 ppm while the uppermost limitation is 2000 ppm[69]. The operation lasted approximately 1.3 h, consuming 3.728 kWh of energy. Notably, the energy consumption of this modular unit was found to be comparable to that of conventional reverse osmosis technology. The advantage of this system lies in the ease of fabricating the carbon electrode and the extended longevity of the membrane used.

Bales et al.[70] developed a CDI sizing model that incorporated process simulations calibrated with experimental data. This model, in conjunction with an agricultural economics model featuring a crop-water-salinity function, was utilized to assess crop yield and farm profitability. Under the constant current model, the CDI simulation data set the feed water salinity at 1500 mg L^{-1} and applied a current of 175 Amps. The resulting purified water had a decreased salinity of approximately 1000 mg L^{-1}. The study

encompassed several fruits and crops such as grapes, apples, and tomatoes. By calculating the internal rate of return and annualized profit for different scenarios, the research demonstrated the economic viability of small-scale on-farm CDI desalination systems that employ brackish groundwater. Furthermore, the application of CDI technology can be optimized based on location-specific information, allowing for efficient and tailored implementation. Similarly, Bales et al.[67] developed a farm-scale economic model to assess the annualized profits of implementing an MCDI desalination system over a 10-year investment period. The study focused on evaluating MCDI system on different crops and their profitability in southeastern Australia, with known groundwater quality. The model served as a tool to estimate the economic viability and potential returns associated with utilizing MCDI to reduce the salinity of the water from 3.2 dS m^{-1} to 1.2 dS m^{-1}. The research highlights the versatility of the MCDI system, which can be tailored to produce different product salinities based on specific crop needs, making it potentially suitable for a wide variety of crops across different regions around the globe.

3.2.2 Hardness. Water hardness refers to the presence of multivalent ions like calcium and magnesium in water. For agricultural irrigation, hard water can cause soil compaction, hinder water drainage, and lead to scaling in irrigation equipment.[71] Thus, softening water is necessary to remove these mineral ions, such as Ca^{2+} and Mg^{2+} (Fig. 1) and further improve soil structure, promote efficient irrigation, and ensure optimal crop growth. For example, the recommend concentration of Mg^{2+} in irrigation water should be less than 50 mg L^{-1}.[69,72] By considering the reported SAC of lab-scale electrodes, the concentration of feed wastewater can be determined, thereby determining the suitability of the electrode for different water desalination applications. van Limpt et al.[73] established a cooling tower for water and hardness ion storage by using MCDI technology with carbon electrode. The results showed that MCDI was effective in reducing the concentration of both Ca^{2+} and Mg^{2+} ions. For high concentration wastewater containing 46 mg L^{-1} Ca^{2+} and 5.1 mg L^{-1} Mg^{2+}, the removal efficiency could reach 74% and 71% respectively, ensuring the application of feed water directly to irrigation. Moreover, Wouters et al.[74] utilized a SiO_2 coated carbon electrode for Ca ions removal. Due to the inducement of hydrophilic surface group, the CDI system exhibited an approximately 98% ion removal efficiency in 2.5mM $CaCl_2$ solution, providing an advanced electrode design method for brackish water desalination with agricultural irrigation application.

3.2.3 Heavy metal. Various anthropogenic activities such as industrial discharges, agricultural runoff and mining operations contribute to the introduction of heavy metals into natural water sources. The presence of heavy metals in agricultural irrigation water poses a significant threat to crop productivity and quality due to their accumulation in soil. This accumulation can result in reduced plant growth, diminished yield, and potential toxicity to humans consuming the affected crops.[75] Consequently, the removal of heavy metals from agricultural irrigation water is imperative to ensure the protection of crops, maintain agricultural productivity, and uphold food safety standards.

Several studies have investigated the effectiveness of CDI for the removal of various heavy metals from different water sources. In the case of arsenic removal, the maximum concentration of the ions for agricultural irrigation water is recommended to be below 100 μg L^{-1}.[69] In recent study a novel titanium oxide/active carbon fiber (TiO_2/ACF) electrode, with a maximum electrosorption capacity of 8.09 mg g^{-1}, efficiently reduced the concentration of As(V) in a 100 μg L^{-1} arsenic solution to below 10 μg L^{-1} within 1.5 hours, meeting WHO drinking water standards.[76] Meanwhile, an AC electrode has demonstrated promising results in the removal of As(V) from water. In an experimental setup with a voltage of 2V and a feed water concentration of 1 mg/L, the AC electrode achieved a high removal efficiency of 98.8%.[77] The high removal efficiency guarantees the feasibility for irrigation water treatment. Gaikwad et al.[78] developed an AC electrode for chromium(VI) adsorption. The maximum adsorption of Cr (VI) reaches over 90 % with 1.2V and below 30 mg L^{-1} initial concentration. The high removal efficiency indicates that this CDI system is an excellent candidate for groundwater heavy metal removal and produce irrigation clean water.[3] For lead removal, the commercial AC electrode has been proved to exhibit over 98% removal efficiency to reduce the concentration below 5 mg L^{-1} (Fig. 5a).[79] This number already fit the recommended concentration (<5 mg L^{-1}) for agricultural usage,[69] it is noticeable that the initial feed water concentration was 100 mg L^{-1}, which is much higher than groundwater Pb concentration.[3] Thus, CDI for Pb^{2+} removal can be applied to treat the waste water from the sources other than ground water.

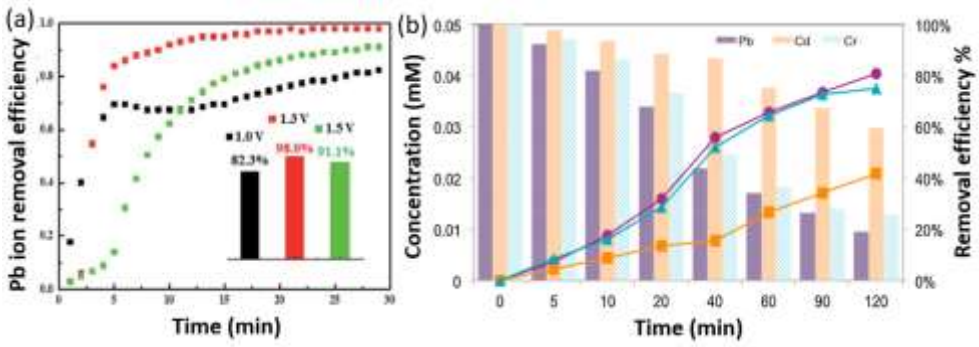

Figure 5. Heavy metal removal in CDI. (a) The removal efficiency of Pb ions at different voltage applied.[79] Copyright 2021 Royal Society of Chemistry. (b) The ion selective of Pb, Cd and Cr removal efficiency.[80] Copyright 2015 Elsevier.

Additionally, the groundwater in nature usually contains more than one single ions.[3] Thus, the ion selectivity is another significant parameter for irrigation water desalination. For example, the removal efficiency of Pb^{2+}, Cd^{2+}, and Cr^{3+} ions follow the order of Pb^{2+} (80.82%) > Cr^{3+} (78.36%) > Cd^{2+} (41.87%) at 1.2V in a mixed solution (Fig. 5b). This can be attributed to the influence of ion size and charge on the desalination process. Generally, ions with higher valence charge and smaller ion radius exhibit a higher affinity for adsorption onto carbon electrodes, resulting in a higher removal efficiency.[80] Thus, a strategy is provided that for real-world brackish water desalination, the concentration of all ions, especially for these with relatively low valence charge and large radius, need to meet the standard for agricultural irrigation.

In summary, these studies collectively underscore the efficacy of CDI as a potential technology for the removal of heavy metals, emphasizing its applicability in wastewater treatment. Heavy metal ions, which usually have higher valence than Na^+, are expected to result in a higher SAC than Na^+. Thus, the porous electrode is more likely to have an ultra-removal efficiency for irrigation water desalination through CDI technology.

3.2.4 Perspective for agricultural irrigation. The application of CDI in agriculture is progressing systematically; however, research on the ultra-high SAC of CDI in agricultural irrigation is relatively limited, with scarcely documented cases. The available cases demonstrate that CDI's ability to efficiently remove a wide range of salt ions from water ensures the provision of a suitable irrigation source with reduced salinity levels, promoting healthier plant growth and preventing soil salinization. The ultra-high SAC of CDI significantly enhances the removal efficiency of salts. Consequently, it becomes evident that CDI, incorporating ultra-high SAC, holds immense potential for agricultural irrigation in the future. By addressing the challenges associated with water scarcity and salinity, the application of ultra-high SAC CDI has the capacity to revolutionize water treatment in irrigation, thereby ensuring sustainable and efficient agricultural production. It is worth pointing out that the fabrication of some high-SAC CDI electrodes involves complex procedures and the use of expensive chemicals, thus leading to high costs of electrode materials. The prospects of CDI in agricultural applications need to be holistically evaluated considering both material performance and electrode costs based on the specific environmental situations.

4. Efficiency and cost analysis for CDI

4.1 Charge efficiency

Charge efficiency (CE) in CDI is an important parameter that quantifies the ratio of the amount of electric charge used to remove salts to the charge supplied to the system during the adsorption period. It is calculated by dividing the amount of salt adsorbed by the total charge transferred, which is influenced by factors such as current and charged duration. Earlier studies suggest that a high CE value typically indicates a low energy consumption, as it reflects the efficiency of charge utilization of the CDI system However, a recent analysis reveals that a high CE value is a necessary but not sufficient condition for an energy-efficient CDI system. We will also need to consider the energy consumed for charge transfer..[81] Thus, when implementing CDI into industrial applications like agriculture irrigation, a high CE, with low charge transfer energy consumption is desirable as it is required to lower overall energy consumption and make the system more energy efficient.

A higher voltage In CDI typically results in a higher CE due to the positive correlation between CE and the diffuse layer potential, which is determined by the cell voltage according to the GCS model.[82] Therefore, higher voltage is desirable for achieving high CE. Another approach to improve CE is the usage of ion exchange membranes (IEMs) between the electrodes. It has been found that MCDI, compared with traditional CDI, has a higher charge efficiency and generally lower energy

consumption. By testing the salt concentration from 20 to 200 mM, Zhao et al.[83] found that the CE of CDI ranges from approximately 55% to 85%, while the CE of MCDI exhibits a much higher number (70% to 100%), leading to a lower energy requirement. Additionally, Shiyong et al.[84] used manganese dioxide (MnO_2) as an intercalation material to prepare a hollow carbon/MnO_2 electrode, which exhibits 25% higher CE than the one without MnO_2. The incorporation of intercalation materials in the electrode design can enhance the CE by facilitating redox reactions, which improves the ion selectivity and reduces the expulsion of ions with the same charge. Meng et al.[85] further coated the carbon cloth electrode with MnO_2 and Ag to increase the pseudocapacitive of the electrode, reaching the total CE of 83%. Therefore, increasing voltage, utilizing IEMs, and incorporating intercalation materials are popular strategies to achieve high CE. Meanwhile, In order to prompt the energy efficiency of the CDI system, which is related to the feed and deionized water concentration, it is significant to improve the SAC of the CDI system. By achieving an ultra-high salt adsorption performance, the CDI system can operate with lower energy consumption, making it more energy-efficient for agricultural applications.[86,87]

4.2 Cost analysis

To determine whether capacitive deionization is feasible for industrial applications, levelized cost of water (LCOW) is regarded as the leading factor in technoeconomic analysis. Several studies have developed models to evaluate the financial viability of CDI including considering operational parameters and capital cost to provide suggestions for technology selection decisions. Capital costs (CAPEX or capital expenditures) include all expenditures to accomplish every step before practical operations, starting from conception, through design, permitting, financing, construction, commissioning, and acceptance testing for proper operation.[88,89] Capital costs include direct and indirect costs. As Ghaffour et al.[90] defined, direct capital costs represent major and auxiliary equipment, associated piping and instrumentation, civil construction for all needed buildings, water intakes and brine discharges infrastructure,. Land costs depend on contractual agreements and may vary from zero to an agreed lump sum payment, depending on site characteristics.[91] Construction costs typically represent 50-85% of the total capital cost. Indirect capital costs usually take a percentage of direct capital cost with 15%-50% representing interest (overheads), working capital, freight and insurance, contingency charges, import duties, project management, and architectural and engineering (A&E) expenses during construction. [88,90,91]

Key variable operating costs (OPEX) include labor, energy, consumables (chemicals, membrane replacement, pump replacement), maintenance and spare parts costs, which depend on facility location in relation to manufacturing and distribution centers.[90] The levelized cost of water (LCOW) or total water cost (TWC) is the sum of capital and operating costs over the contract period. Costs are calculated by dividing the sum of amortized (annualized) capital costs and annual operation and maintenance (O&M) costs by the average annual potable water production.

Hand et al.[92] considered CDI desalination at pilot- and full-scale for technoeconomic analysis. They provided frameworks to estimate various CDI systems with different setups, materials, and operating parameters, and evaluate the desalination performance and system lifespan. Hasseler et al.[93] developed a more normalized open-source program which includes more operational parameters. More complex factors evaluated will result in a more realistic cost estimate. Metzger et al.[94] explored more electrode materials in technoeconomic analysis from capacitive deionization to intercalative deionization. As carbon electrodes store ions capacitively on the porous surface, intercalation electrodes store ions into the materials lattice structure by redox reactions. They found intercalative deionization probably be cost effective for brackish water desalination applications Liu et al.[95] compared the LCOW of reverse osmosis (RO) and several CDI configurations. With 80% water recovery, the estimated specific energy consumption is 0.52 kWh m^{-3} for a cost-minimized RO treatment of a 1500 mg L^{-1} feedwater and LCOW would be 0.12 \$ m^{-3}. The mixing cost to a product water with TDS of 500 mg L^{-1} is included but pretreatment and brine disposal costs are not included. At the Texas Doolittle brackish groundwater desalination plant, the reported LCOW of RO is only 0.33 \$ m^{-3} including pretreatment and brine disposal (2020 value).[96] The LCOW of baseline CDI, MCDI, and flow capacitive deionization (FCDI) are regarded as 0.25, 0.30, and 0.39 \$ m^{-3} under baseline technology assumptions of an electrode lifespan of 0.5 years for CDI and 1 year for MCDI and FCDI (Fig. 6a). To calculate the normalized costs for three configurations, electrode and IEM costs, other capital expenses, electricity costs, and other operating expenses are all taken into consideration. Electrode and electricity cost the most for CDI. IEM costs are the main cost factor for MCDI, consistent with two recent analyses.[92,94] In FCDI, all of the electricity, electrodes and IEMs are important cost drivers.

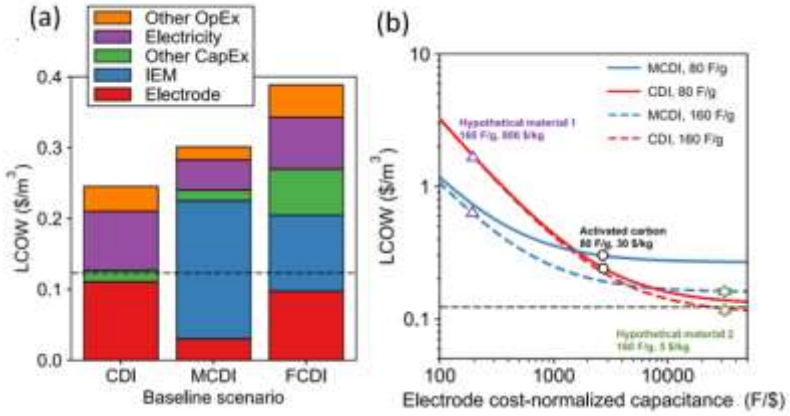

Figure 6. (a) Total component costs for baseline CDI, MCDI, and FCDI. (b) Cost sensitivity of electrode material cost-normalized capacitance. For each line, the specific capacitance is fixed at either 80 or 160 F g^{-1}, and the electrode cost [$ kg^{-1}] varies with cost-normalized capacitance [F $\$^{-1}$].[95] Copyright 2021 American Chemical Society.

Liu et al.[95] further investigated the LCOW of CDI and MCDI systems as a function of cost-normalized capacitance [F $\$^{-1}$] (Fig. 6b). AC and two hypothetical materials are included in the figure for comparison. Increasing the specific capacitance from the current 80 F g^{-1} (activated carbon) to 160 F g^{-1} using expensive electrodes would result in a high LCOW, and the combination of high specific capacitance and low cost would make CDI competitive with RO. However, developing such high-capacitance, low-cost electrode materials may face technical challenges. Overall, their findings suggest that, in addition to increasing specific capacitance, future research on electrode material innovation should aim to prolong electrode lifetime and reduce unit electrode cost. The conclusion is consistent with similar cost analysis studies on the sensitivity of different cost drivers for CDI. Longer system lifetime and stable materials for electrode and membranes will significantly decrease the LCOW. When the actual concentration of brackish water is applied, lifespan is considered as the leading indicator of produced water price in CDI and MCDI. The importance of system lifetime is more pronounced at larger concentration reductions (e.g. by extending system lifespan from 2 to 5 year, water prices in MCDI are reduced from \$0.2-0.65 m^{-3} to \$0.17-0.36 m^{-3} for influent with 2.5 dS m^{-1} and 5 dS m^{-1} salinity.[92] In recent years, significant progress has been made in the development of electrode materials for CDI, focusing on achieving higher adsorption capacity, longer lifespan, and lower cost. These advancements enhance the potential of CDI for industrial applications, particularly in agricultural areas. The properties of these electrode materials, such as the abundance of precursors, simple assembly processes, and general availability contribute to their low-cost nature and facilitate large-scale production, thereby effectively reducing the overall cost of CDI systems used in agriculture.[37,97]

Irrigation, as one of the most feasible applications of CDI, indeed needs intensive cost analysis to demonstrate the potential industrialization. Bales et al.[70] analyzed the low-cost brackish water desalination for irrigated agriculture. Using a farm-scale economics model coupled with a CDI performance model, potentially viable agricultural applications of CDI have been investigated from various crop types and CDI configuration. Scenarios for grapes, oranges, almonds, apples, and tomatoes were modeled to determine the maximum internal rate of return (IRR) and annualized profit (AUD (A$) hectare $(ha)^{-1}$ $year^{-1}$). Groundwater salinity thresholds above which it is considered infeasible to be profitable were 4.2 dS m^{-1} for grapes, 5.5 dS m^{-1} for oranges, 4.4 dS m^{-1} for almonds, 14 dS m^{-1} for apples, and 8.5 dS m^{-1} for tomatoes 60 hectares of crop during the investment period of10 years. Cost calculations for CDI desalinated water depend on the scenario, with a significant number below A$1 kL^{-1}. CDI desalination was found to be economically viable in a range of scenarios and should be further explored as an option to help address global water and food security concerns. Their study shows that compared with reverse osmosis and electrodialysis, it is economically feasible to install small CDI desalination units on farms using brackish groundwater. Pilot studies of CDI desalination in irrigated agriculture will be the next step in determining whether CDI can be part of future irrigation water supply options. Bales et al.[67] developed further accurate crop-water-salinity functions to provide location-based assessments of MCDI desalination for agriculture irrigation. They investigated the profitability of different kinds of crops at different locations (Table 3). From cost breakdown analysis, similar conclusions are made that electrode cost dominates the desalinated water production (Fig. 7). The MCDI system has the flexibility to deliver different product salinities depending on crop requirements, making it ideal for multi-crop farms. Meanwhile, locations factors, especially rainfall, are also important for the profitability of MCDI desalination systems because rainfalls can flush soils and prevent solutes from accumulating in soils when irrigated with brackish water. As a result, , the novel CDI system with advanced ultra-high adsorption performance electrode will be a promising cost-effective desalination method for future agricultural applications.

Table 3 Bore salinity thresholds (dS m^{-1}), lower limit of profitability increase using MCDI compared to irrigation with brackish groundwater (dS m^{-1}), maximum IRR increase (%) and maximum annualized profit increase (\$ ha^{-1} yr^{-1}) for all crops at Clare and the Hunter region.[67] Copyright 2020 Elsevier.

Item	Clare, SA, oranges	Clare, SA, apples	The Hunter, NSW, grapes	The Hunter, NSW, oranges	The Hunter, NSW, apples	The Hunter, NSW, strawberries	The Hunter, NSW, strawberries (glasshouse)
Bore salinity threshold (dS m^{-1})[a]	6.3 (8.2)	9.2 (9.9)	1.8 (3.4)	4.9 (7.2)	8.6 (9.2)	4.3 (6.6)	6.0 (6.9)
Lower limit of profitability increase (dS m^{-1})[a]	3.9 (1.8)	4.7 (1.1)	NA (2.0)	3.6 (1.7)	4.4 (2.2)	3.8 (1.5)	1.2 (1.1)
Maximum IRR increase (%)	10.0	21.4	NA	6.1	17.2	1.6	1.2[b]
Maximum annualized profit increase (\$ ha^{-1} yr^{-1})	\$15,750	\$34,900	\$2500	\$13,750	\$30,850	\$12,750	\$44,200

a First set of numbers is based on internal rate of return (IRR) and number in brackets is based on annualized profit.
b IRR for the glasshouse scenario based on a 50-year investment period due to the high capital cost of the glasshouse.

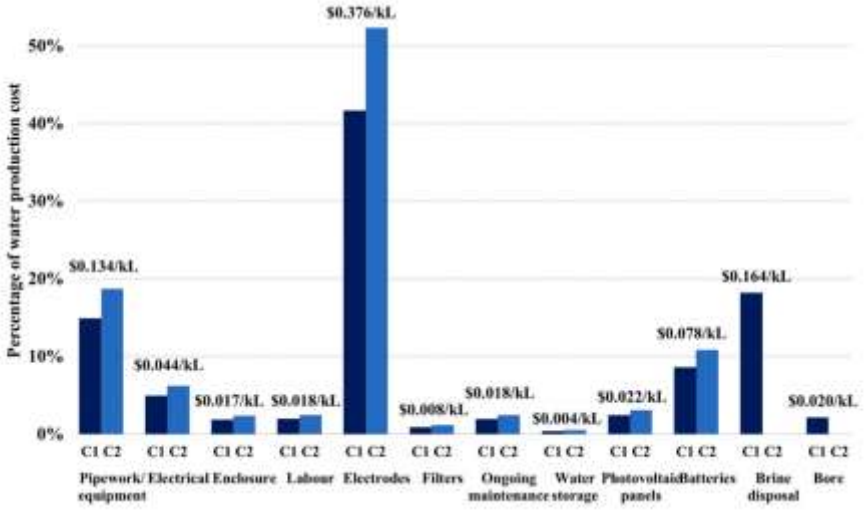

Figure 7. Cost breakdown of the MCDI desalination water production costs for C1, full installation (bore, storage, desalination and brine disposal) and C2, MCDI only (storage and desalination).[67] Copyright 2020 Elsevier.

Conclusions

The ultra-high electrochemical adsorption achieved in CDI system ensures their feasibility in industrial areas. Attaining ultra-high CDI performance can be approached through various means. For example, the material properties, including surface area and capacitance enhanced by chemical activation and advanced materials, as well as the occurrence of faradaic reactions between the electrode and ions, significantly contribute to the superior ion adsorption performance. Meanwhile, we will also need to evaluate the CDI performance based on the real environmental conditions. The recent literature review has shown that such CDI system could be a promising candidate for agricultural applications, in which a thorough investigation of water quality is crucial to control the levels of salt, hardness, and heavy metals within acceptable limits. Due to the high removal efficiency of the ions, CDI is a feasible alternative for irrigation water treatment. Moreover, the charge efficiency and cost of the system must be carefully managed to ensure economic feasibility. Benefiting from ultra-high salt adsorption, superior ion removal efficiency, high charge efficiency and low cost, specifically designed CDI systems could be effectively utilized in the purification of

agricultural irrigation water and hold promise for extension to the treatment of seawater and industrially produced water in the future.

Author Contributions

Investigation, R.H., Y.Y., L.K.; Writing, R.H., Y.Y., L.K.; Review, R.H., Y.Y., L.K., X.L., P.D; Supervision, X.L., and P.D.; Funding Acquisition: X.L., and P.D.

Conflicts of interest

There are no conflicts to declare.

Acknowledgements

This work gratefully acknowledges the financial support from the USDA Department of Agriculture National Institute of Food and Agriculture (AFRI Award Number 2022-67021-36418).

Notes and references

1 Treated Wastewater May Be the Irrigation Wave of the Future, https://www.usda.gov/media/blog/2020/07/21/treated-wastewater-may-be-irrigation-wave-future, (accessed 21 July 2020).
2 S. Singh, N. C. Ghosh, S. Gurjar, G. Krishan, S. Kumar and P. Berwal, *Environ. Monit. Assess.*, 2017, **190**, 29.
3 A. Malakar, D. D. Snow and C. Ray, *Water (Switzerland)*, 2019, **11**, 1–24.
4 K. Balakrishna, A. Rath, Y. Praveenkumarreddy, K. S. Guruge and B. Subedi, *Ecotoxicol. Environ. Saf.*, 2017, **137**, 113–120.
5 T. Asano and J. A. Cotruvo, *Water Res.*, 2004, **38**, 1941–1951.
6 B. J. Selck, G. T. Carling, S. M. Kirby, N. C. Hansen, B. R. Bickmore, D. G. Tingey, K. Rey, J. Wallace and J. L. Jordan, *Water, Air, Soil Pollut.*, 2018, **229**, 186.
7 J. Nolan and K. A. Weber, *Environ. Sci. Technol. Lett.*, 2015, **2**, 215–220.
8 A. Panagopoulos and K.-J. Haralambous, *Mar. Pollut. Bull.*, 2020, **161**, 111773.
9 A. D. Khawaji, I. K. Kutubkhanah and J.-M. Wie, *Desalination*, 2008, **221**, 47–69.
10 K. P. Lee, T. C. Arnot and D. Mattia, *J. Memb. Sci.*, 2011, **370**, 1–22.
11 Y. H. Teow and A. W. Mohammad, *Desalination*, 2019, **451**, 2–17.
12 T. Younos and K. E. Tulou, *J. Contemp. Water Res. Educ.*, 2009, **132**, 3–10.
13 Y. Oren, *Desalination*, 2008, **228**, 10–29.
14 R. He, M. Neupane, A. Zia, X. Huang, C. Bowers, M. Wang, J. Lu, Y. Yang and P. Dong, *Adv. Funct. Mater.*, 2022, **2208040**, 1–10.
15 S. Porada, R. Zhao, A. Van Der Wal, V. Presser and P. M. Biesheuvel, *Prog. Mater. Sci.*, 2013, **58**, 1388–1442.
16 P. Zhang, J. Li and M. B. Chan-Park, *ACS Sustain. Chem. Eng.*, 2020, **8**, 9291–9300.
17 X. Liu, X. Xu, X. Xuan, W. Xia, G. Feng, S. Zhang, Z. G. Wu, B. Zhong, X. Guo, K. Xie and Y. Yamauchi, *J. Am. Chem. Soc.*, 2023, **145**, 9242–9253.
18 Y. Liu, C. Nie, X. Liu, X. Xu, Z. Sun and L. Pan, *RSC Adv.*, 2015, **5**, 15205–15225.
19 M. E. Suss, S. Porada, X. Sun, P. M. Biesheuvel, J. Yoon and V. Presser, *Energy Environ. Sci.*, 2015, **8**, 2296–2319.
20 G. Wang, T. Yan, J. Zhang, L. Shi and D. Zhang, *Environ. Sci. Technol.*, 2020, **54**, 8411–8419.
21 M. Mao, T. Yan, J. Shen, J. Zhang and D. Zhang, *Environ. Sci. Technol.*, 2021, **55**, 7665–7673.
22 M. Mao, T. Yan, J. Shen, J. Zhang and D. Zhang, *Environ. Sci. Technol.*, 2021, **55**, 3333–3340.
23 G. Wang, T. Yan, J. Shen, J. Zhang and D. Zhang, *Environ. Sci. Technol.*, 2021, **55**, 11979–11986.
24 S. D. Datar, R. Mane and N. Jha, *Water Environ. Res.*, 2022, **94**, e10696.
25 Z. Y. Yang, L. J. Jin, G. Q. Lu, Q. Q. Xiao, Y. X. Zhang, L. Jing, X. X. Zhang, Y. M. Yan and K. N. Sun, *Adv. Funct. Mater.*, 2014, **24**, 3917–3925.
26 Y. Jiang, Z. Hou, L. Yan, H. Gang, H. Wang and L. Chai, *Polymers (Basel).*, 2022, **14**, 4776.
27 Z. Chen, X. Xu, Z. Ding, K. Wang, X. Sun, T. Lu, M. Konarova, M. Eguchi, J. G. Shapter, L. Pan and Y. Yamauchi, *Chem. Eng. J.*, 2021, **407**, 127148.
28 J. Ma, Y. Cheng, L. Wang, X. Dai and F. Yu, *Chem. Eng. J.*, 2020, **384**, 123329.
29 Z. Gengmao, S. K. Mehta and L. Zhaopu, *Agric. Water Manag.*, 2010, **97**, 1987–1993.
30 J. M. Beltrán, *Agric. Water Manag.*, 1999, **40**, 183–194.

31 G. Liu, L. Qiu, H. Deng, J. Wang, L. Yao and L. Deng, *Appl. Surf. Sci.*, 2020, **524**, 146485.
32 J. Yan, H. Zhang, Z. Xie and J. Liu, *AIP Conf. Proc.*, 2017, **1864**, 020218-1–020218-6.
33 G. Wang, C. Pan, L. Wang, Q. Dong, C. Yu, Z. Zhao and J. Qiu, *Electrochim. Acta*, 2012, **69**, 65–70.
34 Y. Zhang, L. Chen, S. Mao, Z. Sun, Y. Song and R. Zhao, *J. Colloid Interface Sci.*, 2019, **536**, 252–260.
35 Z. Zhang, Y. Zhang, C. Jiang, D. Li, Z. Zhang, K. Wang, W. Liu, X. Jiang, Y. Rao, C. Xu, X. Chen and N. Meng, *Desalination*, 2022, **529**, 115653.
36 J. Oladunni, J. H. Zain, A. Hai, F. Banat, G. Bharath and E. Alhseinat, *Sep. Purif. Technol.*, 2018, **207**, 291–320.
37 X. Xu, Z. Sun, D. H. C. Chua and L. Pan, *Sci. Rep.*, 2015, **5**, 1–9.
38 X. Xu, T. Yang, Q. Zhang, W. Xia, Z. Ding, K. Eid, A. M. Abdullah, M. Shahriar A. Hossain, S. Zhang, J. Tang, L. Pan and Y. Yamauchi, *Chem. Eng. J.*, 2020, **390**, 124493.
39 Z. Xing, X. Xuan, H. Hu, M. Li, H. Gao, A. Alowasheeir, D. Jiang, L. Zhu, Z. Li, Y. Kang, J. Zhang, X. Yi, Y. Yamauchi and X. Xu, *Chem. Commun.*, 2023, **59**, 4515–4518.
40 S. Wang, N. Gao, G. Wang, C. He, S. Lv and J. Qiu, *Desalination*, 2021, **520**, 115341.
41 W. Shi, H. Li, X. Cao, Z. Y. Leong, J. Zhang, T. Chen, H. Zhang and H. Y. Yang, *Sci. Rep.*, 2016, **6**, 1–9.
42 J. Ma, L. Wang and F. Yu, *Electrochim. Acta*, 2018, **263**, 40–46.
43 S. Vafakhah, G. J. Sim, M. Saeedikhani, X. Li, P. Valdivia Y Alvarado and H. Y. Yang, *Nanoscale Adv.*, 2019, **1**, 4804–4811.
44 J. Guo, X. Xu, J. P. Hill, L. Wang, J. Dang, Y. Kang, Y. Li, W. Guan and Y. Yamauchi, *Chem. Sci.*, 2021, **12**, 10334–10340.
45 Q. He, R. He, A. Zia, G. Gao, Y. Liu, M. Neupane, M. Wang, Z. Benedict, K. K. Al-Quraishi, L. Li, P. Dong and Y. Yang, *Small*, 2022, **384**, 2200272.
46 J. Cao, Y. Wang, L. Wang, F. Yu and J. Ma, *Nano Lett.*, 2019, **19**, 823–828.
47 F. Chen, Y. Huang, L. Guo, L. Sun, Y. Wang and H. Y. Yang, *Energy Environ. Sci.*, 2017, **10**, 2081–2089.
48 J. Elisadiki and C. K. King'ondu, *J. Electroanal. Chem.*, 2020, **878**, 114588.
49 Y. Zhang, H. Li, Q. Yang, S. Zhang, B. Zhao, J. Wu, N. Shang, X. Zhao, Z. Xiao, X. Zang, J. Kim, X. Xu and Y. Yamauchi, *J. Mater. Chem. A*, 2023, 14356–14365.
50 K. Wang, Y. Liu, Z. Ding, Y. Li, T. Lu and L. Pan, *J. Mater. Chem. A*, 2019, **7**, 12126–12133.
51 Z. Yue, T. Gao and H. Li, *Desalination*, 2019, **449**, 69–77.
52 Y. Liu, X. Gao, Z. Wang, K. Wang, X. Dou, H. Zhu, X. Yuan and L. Pan, *Chem. Eng. J.*, 2021, **403**, 126326.
53 Y. Zhao, B. Liang, X. Wei, K. Li, C. Lv and Y. Zhao, *J. Mater. Chem. A*, 2019, **7**, 10464–10474.
54 S. Gong, H. Liu, F. Zhao, Y. Zhang, H. Xu, M. Li, J. Qi, H. Wang, C. Li, W. Peng, X. Fan and J. Liu, *ACS Nano*, 2023, **17**, 4843–4853.
55 N. Liu, L. Yu, B. Liu, F. Yu, L. Li, Y. Xiao, J. Yang and J. Ma, *Adv. Sci.*, 2023, **10**, 1–10.
56 X. Xu, M. Eguchi, Y. Asakura, L. Pan and Y. Yamauchi, *Energy Environ. Sci.*, 2023, 1815–1820.
57 X. Xu, J. Tang, Y. V. Kaneti, H. Tan, T. Chen, L. Pan, T. Yang, Y. Bando and Y. Yamauchi, *Mater. Horizons*, 2020, **7**, 1404–1412.
58 S. Zhang, X. Xu, X. Liu, Q. Yang, N. Shang, X. Zhao, X. Zang, C. Wang, Z. Wang, J. G. Shapter and Y. Yamauchi, *Mater. Horizons*, 2022, **9**, 1708–1716.
59 J. M. Valente Nabais, J. G. Teixeira and I. Almeida, *Bioresour. Technol.*, 2011, **102**, 2781–2787.
60 J. V. Nabais, P. Carrott, M. M. L. Ribeiro Carrott, V. Luz and A. L. Ortiz, *Bioresour. Technol.*, 2008, **99**, 7224–7231.
61 A. Aworn, P. Thiravetyan and W. Nakbanpote, *J. Anal. Appl. Pyrolysis*, 2008, **82**, 279–285.
62 J. M. V. Nabais, P. Nunes, P. J. M. Carrott, M. M. L. Ribeiro Carrott, A. M. García and M. A. Díaz-Díez, *Fuel Process. Technol.*, 2008, **89**, 262–268.
63 A. E. Ismanto, S. Wang, F. E. Soetaredjo and S. Ismadji, *Bioresour. Technol.*, 2010, **101**, 3534–3540.
64 X. Li, W. Xing, S. Zhuo, J. Zhou, F. Li, S.-Z. Qiao and G.-Q. Lu, *Bioresour. Technol.*, 2011, **102**, 1118–1123.
65 P. González-García, T. A. Centeno, E. Urones-Garrote, D. Ávila-Brande and L. C. Otero-Díaz, *Appl. Surf. Sci.*, 2013, **265**, 731–737.
66 W. Xing, J. Liang, W. Tang, D. He, M. Yan, X. Wang, Y. Luo, N. Tang and M. Huang, *Desalination*, 2020, **482**, 114390.
67 C. Bales, B. Lian, J. Fletcher, Y. Wang and T. D. Waite, *Desalination*, 2021, **502**, 114913.
68 M. Elshafei, A. M. Amer, A. Seleym, Z. Khalifa and T. S. Ahmed, *Desalin. Water Treat.*, 2020, **193**, 11–18.
69 R. S. Ayers and D. W. Westcot, *Water quality for agriculture*, Food and Agriculture Organization of the United Nations Rome, 1985, vol. 29.
70 C. Bales, P. Kovalsky, J. Fletcher and T. D. Waite, *Desalination*, 2019, **453**, 37–53.
71 C. Gabrielli, G. Maurin, H. Francy-Chausson, P. Thery, T. T. M. Tran and M. Tlili, *Desalination*, 2006, **201**, 150–163.
72 Water Quality for Crop Production, https://ag.umass.edu/greenhouse-floriculture/greenhouse-best-management-practices-bmp-manual/water-quality-for-crop.
73 B. Van Limpt and A. van der Wal, *Desalination*, 2014, **342**, 148–155.
74 J. J. Wouters, M. I. Tejedor-Tejedor, J. J. Lado, R. Perez-Roa and M. A. Anderson, *J. Electrochem. Soc.*, 2018, **165**, E148–E161.
75 F. Fu and Q. Wang, *J. Environ. Manage.*, 2011, **92**, 407–418.
76 L. Peng, Y. Chen, H. Dong, Q. Zeng, H. Song, L. Chai and J. Gu, *Water, Air, Soil Pollut.*, 2015, **226**, 203.
77 J.-Y. Lee, N. Chaimongkalayon, J. Lim, H. Y. Ha and S.-H. Moon, *Water Sci. Technol.*, 2016, **73**, 3064–3071.
78 M. S. Gaikwad and C. Balomajumder, *Sep. Purif. Technol.*, 2017, **186**, 272–281.

79 Y. Gui and D. J. Blackwood, *RSC Adv.*, 2021, **11**, 12877–12884.
80 Z. Huang, L. Lu, Z. Cai and Z. J. Ren, *J. Hazard. Mater.*, 2016, **302**, 323–331.
81 L. Wang, J. E. Dykstra and S. Lin, *Environ. Sci. Technol.*, 2019, **53**, 3366–3378.
82 R. Zhao, P. M. Biesheuvel, H. Miedema, H. Bruning and A. van der Wal, *J. Phys. Chem. Lett.*, 2010, **1**, 205–210.
83 R. Zhao, P. M. Biesheuvel and A. van der Wal, *Energy Environ. Sci.*, 2012, **5**, 9520–9527.
84 S. Wang, G. Wang, T. Wu, C. Li, Y. Wang, X. Pan, F. Zhan, Y. Zhang, S. Wang and J. Qiu, *Environ. Sci. Technol.*, 2019, **53**, 6292–6301.
85 M. Li and H. G. Park, *ACS Appl. Mater. Interfaces*, 2018, **10**, 2442–2450.
86 S. K. Patel, C. L. Ritt, A. Deshmukh, Z. Wang, M. Qin, R. Epsztein and M. Elimelech, *Energy Environ. Sci.*, 2020, **13**, 1694–1710.
87 L. Wang, J. E. Dykstra and S. Lin, *Environ. Sci. Technol.*, 2019, **53**, 3366–3378.
88 M. Wilf and L. Awerbuch, *The guidebook to membrane desalination technology : reverse osmosis, nanofiltration and hybrid systems : process, design, applications and economics*, 2007.
89 R. Huehmer, J. Gomez, J. Curl and K. Moore, *COST MODELING OF DESALINATION SYSTEMS*, 2011.
90 N. Ghaffour, T. M. Missimer and G. L. Amy, *Desalination*, 2013, **309**, 197–207.
91 H. Ettouney, H. El-Dessouky, R. S. Faibish and P. J. Gowin, *Chem. Eng. Prog.*, 2002, **98**, 32–39.
92 S. Hand, J. S. Guest and R. D. Cusick, *Environ. Sci. Technol.*, 2019, **53**, 13353–13363.
93 T. D. Hasseler, A. Ramachandran, W. A. Tarpeh, M. Stadermann and J. G. Santiago, *Water Res.*, 2020, **183**, 116034.
94 M. Metzger, M. M. Besli, S. Kuppan, S. Hellstrom, S. Kim, E. Sebti, C. V Subban and J. Christensen, *Energy Environ. Sci.*, 2020, **13**, 1544–1560.
95 X. Liu, S. Shanbhag, T. V Bartholomew, J. F. Whitacre and M. S. Mauter, *ACS ES&T Eng.*, 2021, **1**, 261–273.
96 J. Arroyo and S. Shirazi, *Texas Water Dev. Board*, 2012, 1–7.
97 H. Zhang, J. Tian, X. Cui, J. Li and Z. Zhu, *Carbon N. Y.*, 2023, **201**, 920–929.

